UC San Diego

UC San Diego Previously Published Works

Title

A universal biventricular coordinate system incorporating valve annuli: Validation in congenital heart disease

Permalink

https://escholarship.org/uc/item/4pn030px

Journal

Medical Image Analysis, 93

ISSN

1361-8415

Authors

Pankewitz, Lisa

Hustad, Kristian G

Govil, Sachin

et al.

Publication Date

2024-04-01

DOI

10.1016/j.media.2024.103091

Peer reviewed

eScholarship.org Powered by the California Digital Library
University of California

Author Manuscript

Author Manuscript

Author Manuscript

Author Manuscript

HHS Public Access

Author manuscript

Med Image Anal. Author manuscript; available in PMC 2025 April 01.

Published in final edited form as:

Med Image Anal. 2024 April ; 93: 103091. doi:10.1016/j.media.2024.103091.

A universal biventricular coordinate system incorporating valve annuli: Validation in congenital heart disease

Lisa Pankewitz[a,b], **Kristian G Hustad**[a], **Sachin Govil**[c], **James C Perry**[c,d], **Sanjeet Hegde**[d], **Renxiang Tang**[c], **Jeffrey H Omens**[c,e], **Alistair A Young**[f], **Andrew D McCulloch**[c,e,*], **Hermenegild J Arevalo**[a]

[a]Simula Research Laboratory, Kristian Augusts gate 23, 0164 Oslo, Norway

[b]Department of Informatics, University of Oslo, Gaustadalléen 23B, 0373 Oslo, Norway

[c]Department of Bioengineering, University of California San Diego, 9500 Gilman Drive, La Jolla, CA, 92093-0412, USA

[d]Department of Pediatrics, University of California San Diego, La Jolla, CA, USA

[e]Department of Medicine, University of California San Diego, La Jolla, CA, USA

[f]School of Biomedical Engineering & Imaging Sciences, King's College London, London, UK

Abstract

Universal coordinate systems have been proposed to facilitate anatomic registration between three-dimensional images, data and models of the ventricles of the heart. However, current universal ventricular coordinate systems do not account for the outflow tracts and valve annuli where the topology is complex. Here we propose a modification to the 'Cobiveco' biventricular coordinate system that automatically accounts for the intervalvular bridges of the base and provides a tool for anatomically consistent registration between widely varying biventricular shapes. CobivecoX uses a novel algorithm to separate intervalvular bridges and assign new coordinates, including an inflow-outflow coordinate, to describe local positions in these regions uniquely and consistently. Anatomic consistency of registration was validated using curated three-dimensional biventricular shape models derived from cardiac MRI measurements in patients with congenital heart diseases. This new method allows the advantages of universal cardiac coordinates to be used for three-dimensional ventricular imaging data and models that include the left and right ventricular outflow tracts and valve annuli.

Graphical Abstract

[*]Corresponding author: amcculloch@ucsd.edu (Andrew D McCulloch).

Author contributions

Lisa Pankewitz: Conceptualization, Methodology, Software, Visualization, Writing- Original draft preparation, Reviewing and Editing., **Kristian G Hustad**: Software, **Sachin Govil**: Methodology, **James C Perry**: Supervision, Funding acquisition, **Sanjeet Hegde**: Supervision, Funding acquisition, **Renxiang Tang**: Methodology, **Jeffrey H Omens**: Supervision, Funding acquisition, **Andrew D McCulloch**: Supervision, Funding acquisition, **Hermenegild J Arevalo**: Supervision, Funding acquisition

Declaration of generative AI in scientific writing

During the preparation of this work the author(s) used Chat-GPT in order to rephrase and grammar check sentences as well as to trouble shoot a plot. After using this tool/service, the author(s) reviewed and edited the content as needed and take(s) full responsibility for the content of the publication.

Author Manuscript Author Manuscript Author Manuscript Author Manuscript

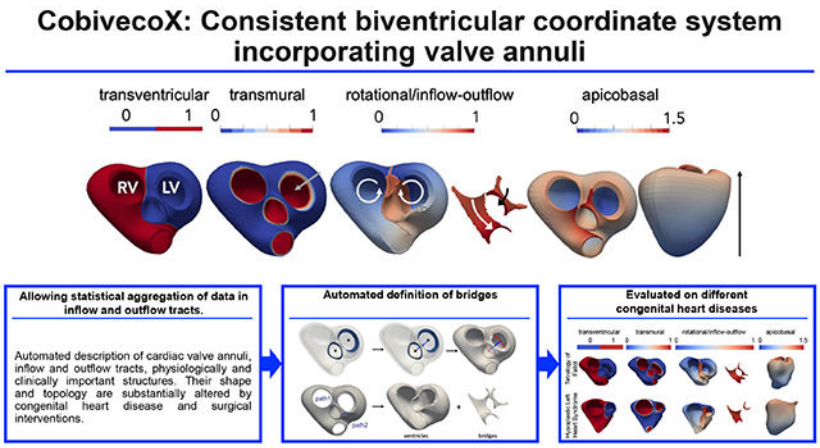

Keywords

Cardiac geometry; Coordinates; Congenital Heart Disease; Mapping; 41A05; 41A10; 65D05; 65D17

1. Introduction

Three-dimensional cardiac imaging data sets and models are increasingly being used for precision medicine, patient-specific modeling and population analysis (Peirlinck et al. (2021); Niederer et al. (2019, 2020)). While four-chamber descriptions of anatomy are the most complete, most clinical research and analysis uses one- or two-chamber reconstructions of atrial or ventricular anatomy.

Statistically summarizing or comparing spatially varying ventricular shape or properties between individuals or registering three-dimensional measurements to models is simplified and standardized by the use of universal cardiac coordinate systems (Schuler et al. (2021); Bayer et al. (2018)). However, current universal biventricular coordinates do not account for the topologically complex inflow and outflow tracts at the base of the ventricles, or they require coordinates in the outflow tracts and valve annuli to be assigned manually even though these structures are clinically important and notably variable Cheung et al. (2019); Anderson et al. (2019); Aras et al. (2022). Moreover, some automated methods are sensitive to geometric variations such as wall thickness (Schuler et al. (2021); Bayer et al. (2018); Doste et al. (2019)). The cardiac valve annuli, inflow and outflow tracts, and their fibrous skeleton are developmentally and physiologically important structures whose shape and topology is substantially altered in a variety of congenital heart diseases and surgical interventions Anderson et al. (2016); Kirby and Waldo (1995); van Gils (1981); Cheung et al. (2019); Anderson et al. (2019); Kapel et al. (2017); Hickey et al. (2009); Kirklin et al. (1989). These structures, such as the fibrous valve skeleton, may be important for diagnosis or planning clinical interventions. Therefore, we have developed a new tool for generating a biventricular coordinate system that takes into account the anatomy of the valve annuli, yielding unique coordinates within the intervalvular bridges.

Author Manuscript Author Manuscript Author Manuscript Author Manuscript

We modified the existing Cobiveco coordinate system Schuler et al. (2021) that is based on the trajectory distance method, to make it robust to a broader range of cardiac geometries. We then extended the existing system to define intervalvular bridges automatically. We demonstrate that the system is reliable when applied to congenital heart diseases (CHD), including severe lesions such as hypoplastic left heart syndrome (HLHS), which pose extra challenges owing to severe developmental abnormalities in cardiac morphology.

2. Methodology

2.1. General description

CobivecoX extends the previously published Cobiveco consistent biventricular coordinate system for ventricular geometries by accounting for the four valve annuli (Schuler et al., 2021). CobivecoX coordinates in the ventricles are defined separately in the ventricular and intervalvular bridges. As in Cobiveco, anatomic position is defined as a tuple of four coordinates. If not stated otherwise, the calculation of the coordinates followed the original steps (Schuler et al., 2021).

CobivecoX was implemented in open-source MATLAB code. The source code also includes a set of pre-processing scripts to automatically create the input surface files needed to apply CobivecoX on a given tetrahedral volumetric mesh. CobivecoX was designed to be backwards compatible with Cobiveco 1.0.

2.2. Input definition

The CobivecoX calculations use a biventricular tetrahedral volume with four valve annuli (the mitral valve annulus, the tricuspid valve annulus, the aortic valve annulus and pulmonary valve annulus) and boundary surfaces including an epicardial surface with base, epicardial surface without base, the left ventricular (LV) endocardium, the right ventricular (RV) endocardium, the mitral valve annulus, the tricuspid valve annulus, the aortic valve annulus and pulmonary valve annulus as shown in Figure 1. If these surfaces have not been manually defined, the CobivecoX code can extract them semi-automatically by using region-growing from manually specified seed points. Note, that the definition of left and right and anterior and posterior is based on the input. The patients left and right side however, can be reversed in certain pathologies.

2.3. Computation of the transventricular and transmural coordinates

The transventricular coordinate (*tv*) is a binary coordinate defining the left and right ventricles. To calculate *tv*, we follow the steps previously described in (Schuler et al., 2021). In short, we determine the solution to Laplace's equation with boundary conditions of 0 at the RV endocardium and 1 at the LV endocardium. The result is rounded to the closest integer to yield *tv* and can be seen in Figure 2. A remeshing step, the first of three, ensures the separation of *tv* between the left and right ventricle, avoiding elements to be placed on the boundary.

A prerequisite for calculating the transmural coordinate (*tm*) is assigning a septal surface, which is the surface between the RV and LV. To do so, all the tetrahedron faces on the

Author Manuscript Author Manuscript Author Manuscript Author Manuscript

boundary between RV and LV are extracted yielding the septal surface and the septal curve. The septal curve represents the points of the septal surface intersecting the epicardium. After identifying the septal surface, *tm* is calculated as described previously (Schuler et al., 2021). In short, the solution to the Laplace equation with boundary conditions $tm = 0$ at the septal and epicardial surfaces, and $tm = 1$ at the endocardial surfaces, is computed. Thereafter, *tm* is calculated by trajectory projection along the gradient of the Laplacian solution. The final *tm* is shown in Figure 2.

2.4. Extraction of the Global Heart Axes

A orthogonal, global heart coordinate system is required to define the apex of the biventricular mesh. The global heart axes and apex point are defined as described previously (Schuler et al., 2021).

The first of three global heart axes, $v_{LongAxis}$, is the vector most orthogonal to the normals of the LV endocardial surface and directed from base to apex. The second axis, referred to as $v_{LeftRight}$, is determined based on the surface normal of the flattest part of the septal surface. To extract the flattest part of the septal surface, a plane is fitted to the septal surface determining the major directions of the plane. The major directions are described by $v_{LongAxis}$ for the apico-basal extension of the septal surface and an anterior-posterior direction, determined by the cross product of the vector normal to the septal surface and $v_{LongAxis}$. The determined directions are used to extract the non-curved part of the septal surface by truncating it by 15% at the basal side in the directions of the long axis as well as 20% and 10% at the anterior and posterior side, respectively (Fig. 3). Based on the truncated septal surface the normal vector is determined, which is orthogonalized to $v_{LongAxis}$, yielding $v_{LeftRight}$.

Lastly, the third global heart axis, $v_{AnteriorPosterior}$, is defined as the cross product of $v_{LongAxis}$ with $v_{LeftRight}$.

2.5. Remeshing step number 2

Before the rotational coordinate can be calculated, correct boundary surfaces need to be defined. Therefore, a second remeshing step is needed to extract the boundary surfaces at the interventricular junctions (Schuler et al., 2021). The remeshing follows the steps previously described by Schuler et al. (2021). First, the solution to the Laplace equation is calculated with boundary conditions of 0 at the epicardium and 1 at the septal surface. Then a remeshing step with an isovalue discretization at 0.5 of the Laplacian solution is performed, to result in a free wall volume, a septal volume, and an interjunctional surface. The interjunctional surface represents the elements that are part of the septal volume but intersect with the epicardium. This interjunctional surface is then split into an anterior and posterior part, yielding the boundary surfaces required for the calculation of the rotational coordinate.

Author Manuscript Author Manuscript Author Manuscript Author Manuscript

2.6. Automated separation of intervalvular bridges from the biventricular volumetric mesh

To calculate the next set of coordinates, the biventricular model is first split into the intervalvular bridges and the ventricular region. Then the following coordinates were calculated: the rotational coordinate (*rt*) and the apicobasal coordinate (*ab*) on the ventricular regions, and the *ab* and inflow-outflow coordinate (*io*) on the intervalvular bridges..

Figure 4 outlines the steps to automatically identify the intervalvular bridges. First the center of each valve annulus surface is calculated. Within each individual ventricle, the vector connecting the center of the inflow and outflow valve plane is calculated. This vector is then projected into the respective valve plane and serves as a reference vector for both valves in one ventricle. Two points for each valve annulus were identified by rotating the reference vector +70 and −70 degrees around the valve plane normal for all annuli except for the first tricuspid valve, where a rotation of +75 and −20 degrees is applied. These points served as the starting points to calculate the shortest path between the inflow and outflow valve annuli in each ventricle separately.

To calculate the shortest path between the starting point on the inflow valve annulus and the starting point on the outflow valve annulus in each ventricle individually, subgraphs were created. The subgraphs for LV and RV endocardium exclude the septum as well as the opposite ventricle. Within these subgraphs the shortest path between the inflow and outflow valve annuli are calculated, with one path using the starting points on the inflow and outflow valve annuli closer to the free wall of the ventricle and the other one using the starting points closer to the septum to calculate the shortest path. The result are two paths in each subgraph in the endocardium, a path closer to the free wall and a path closer to the septum. In total, four shortest paths are calculated in each ventricle, which outline one intervalvular region in each ventricle. Planes are then fitted to the paths which are used to separate the intervalvular bridges from the ventricles.

2.7. Calculate the rotational and the inflow-outflow coordinates

The *rt* was calculated using the trajectory projection as previously described in Cobiveco 1.0 (Schuler et al., 2021). The final *rt* on the ventricles is scaled to range from 0 to $\frac{6}{7}$. Ranging from 0 to $\frac{4}{7}$ in the free walls and $\frac{4}{7}$ to $\frac{6}{7}$ in the septal wall (Fig. 6).

The *io*, the complementing coordinate of the *rt* in the intervalvular bridges, is determined by the trajectory projection between the inflow valve annulus, serving as a boundary condition of 0, and the outflow valve annulus, serving as a boundary condition of 1 in each ventricle (Fig. 5). The final *io* is scaled to range from $\frac{6}{7}$ to 1 (Fig. 6).

2.8. Calculate the apicobasal coordinate

The *ab* was calculated using the trajectory projection as previously described in Cobiveco 1.0 with the modification of the base surfaces as the boundary conditions for calculating the apicobasal Laplacian (Schuler et al., 2021). The apex point and base surface are set as boundary conditions. The base is defined as the surfaces which intersect with the removed

Author Manuscript Author Manuscript Author Manuscript Author Manuscript

intervalvular bridges and the valve annuli regions on the ventricular volume (Fig. 5). While the apex point boundary is set to 0, the basal boundary is set to 1.

In short, *ab* is defined by calculating apicobasal curves created from extracted isocontours at distinct values of the rotational and transmural coordinates. Throughout these curves the normalized distance is calculated. The final *ab* on the ventricles is scaled to have values from 0 to 1 (Figure 7).

The *ab* on the intervalvular bridges is also defined using trajectory projection. The boundary surface of the *ab* closer to the free wall is set to 0 while the boundary surface closer to the septum were set to 1 in each ventricle respectively (Fig. 5). The final *ab* in the intervalvular bridges is scaled from 1 to 1.5 (Figure 7).

3. Evaluation

3.1. Test geometries

To evaluate CobivecoX, we use a digital cohort of biventricular shapes created from a statistical shape atlas of Tetralogy of Fallot (TOF) patients, as well as a cohort of patient specific geometries of TOF and hypoplastic left heart syndrome (HLHS) patients.

3.1.1. Creation of patient specific models of TOF and HLHS patients—TOF and HLHS specific geometries were derived as described previously (Govil et al., 2023; Mauger et al., 2021). In short, cardiac magnetic resonance images were obtained as part of standard clinical practice. 1.5T MRI Siemens Avanto (Siemens Medical Systems) and GE Discovery (GE Healthcare Systems) were used. Short-axis slices were acquired traversing both ventricles from apex to base, parallel to the tricuspid valve plane. Long-axis slices were acquired in LV outflow tract, RV outflow tract, 4-chamber heart as well as 2-chamber heart views. Additionally, cine images were obtained during breath-hold using steady-state free procession imaging.

To create the models, an expert drew contours at end-diastole on both short-axis and long-axis cine slices using the software Segment (medviso), excluding the papillary muscles. For the following shape analysis, landmark points for the aortic, pulmonary, mitral and tricuspid valve were defined. Meshes were generated based on a previously created biventricular subdivision surface template. It has to be noted, that different biventricular topologies and subdivision surface templates were used for the HLHS and TOF patients. The mesh included epicardium, RV and LV endocardium, as well as all four valve planes. Using an iterative registration algorithm, the template mesh is automatically customized to each patient and corrected for breath-hold artefacts. Using the landmarks defined by the expert, the valve locations were customized via landmark registration. Diffeomorphic non-rigid registration is used to personalize the surfaces to the manually defined contours.

For the geometries in this article, data of 110 TOF and 2 HLHS patients were obtained retrospectively from the clinical centers Rady Children’s Hospital, San Diego, CA, US and The Center for Advanced Magnetic Resonance Imaging, Auckland, NZ with approval from

Author Manuscript Author Manuscript Author Manuscript Author Manuscript

local institutional review boards via waiver of informed consent (UCSD IRB 201138 and HDEC 16/STH/248, respectively).

The patient specific geometries of HLHS were based on two anonymized patients younger than 5 months. The HLHS patient geometries are shown in Figure 8.

Models used for the creation of the TOF shape atlas, included patients aged 20 ± 12 years (66 male, 44 female).

The biventricular TOF atlas is created in end diastole (ED) shape. First, patient-specific ED surface points were aligned to the population mean of the ED surface points by a rigid registration. Second, alignment of points is used. Shape variations across the TOF population were evaluated using principal component analysis.

Finally, a subcohort of 10 patient specific TOF models was created from the 110 patient specific TOF models.

3.2. Creation of atlas-based digital cohort

For this study, 500 semi-random instances of the statistical shape-model were created. The first 40 shape modes of the atlas were sampled, according to the variance they represent in the TOF population. For example, mode 1 explains approximately 41 percent of the variation observed in the atlas. Hence, 208 instances were created based on mode one. The 208 instances were created by sampling evenly within three standard deviations of mode 1. This was performed similarly for modes 2-24. Figure 9, shows an example of the geometries created for modes 1 and 24 within 3 standard deviations from the mean shape of the atlas.

3.3. Creation of tetrahedral meshes

All meshes were tetrahelized and meshed to the desired element size of 350 to 450 μm using Gmsh (Geuzaine and Remacle, 2009).

3.4. Evaluation of mapping errors

The two-way mapping error is a quantitative measure to evaluate cardiac coordinates described by (Bayer et al., 2018). This mapping error is calculated using the coordinate system to map Euclidean coordinates from one heart to another and then back to the initial heart. The difference between the original and mapped Euclidean coordinates is then calculated on the first heart in mm, with 0 mm being the ideal result.

4. Results

4.1. Two-way mapping errors

The two-way mapping errors as described in Section 3.4 were calculated between the mean shape model of the TOF atlas to all instances of the atlas, and all patient specific models. The errors were averaged by the number of mappings for each subcohort or atlas.

4.1.1. Two-way mapping errors in the patient specific TOF cohort—To demonstrate the versatility of CobivecoX for vastly different geometries within CHD, we

Author Manuscript Author Manuscript Author Manuscript Author Manuscript

assigned CobivecoX to patient specific geometries of different pathologies. First, CobivecoX was assigned on 10 patient specific TOF meshes. For one patient specific TOF geometry, the matrix factorization failed and hence the final coordinates could not be created successfully. The resulting coordinates are visualized in Figure 10 and S1. The statistical measures for determining the two-way mapping error in this cohort are shown in Table 1.

Median, mean and 90th percentile resulted in 0.02 mm, 0.08 mm and 0.12 mm in the complete biventricular geometry.

4.1.2. Two-way mapping errors in the patient specific HLHS cohort—

We assigned CobivecoX on 2 patient specific meshes of the rare congenital heart disease HLHS, a single ventricle disease (Fig. 10). The statistical measures for the mapping are shown in Table 1. Median, mean, 90th and 99th percentile were determined to be 0.08 mm, 0.3 mm, 0.58 mm and 4.37 mm respectively.

4.2. Two-way mapping errors in the TOF atlas cohort

CobivecoX was successfully computed on 481 of 500 instances of the TOF atlas. Out of 500 instances created, 11 instances failed to be created in Gmsh due to segment-facet intersections or overlapping facets. Of the remaining 489 instances 8 could not be assigned correctly due to a failed matrix factorization or wrongly assigned boundary conditions in the RV bridge leading to an unsuccessful or incorrect creation of the final coordinates. The final coordinates are visualized in the supplementary videos that can be observed in the electronic version of this article. The statistical measures observed for calculating the two-way mapping errors between the mean shape of the TOF atlas and all instances of the TOF atlas are summarized in Table 1. The mapping accuracy in the bridge regions is determined with a mean error of 0.09±0.33 mm (Table 1). The mean mapping error shows a mean error of 0.07 ± 0.25 mm. The median resulted in 0.02 mm. The local distribution of the observed two-way mapping errors within the atlas cohort is visualized on the mean shape of the atlas in Figure 11. An increase of mapping errors can be observed at the interventricular junctions and intervalvular bridges between the RV and LV (Figure 11).

4.3. Relationship of two-way mapping error and size of heart

To investigate the dependence of the mapping error on anatomical changes, we used the atlas cohort to investigate the influence of the modes, and z-score e.g. the distance of the respective instance from the mean on the two-way mapping error (3.1.1). Mode 1 is the mode that largely represents changes in the size and the volume of the TOF hearts. Therefore, if we sample mode 1 from −3 to +3 standard deviations from the mean shape we will observe the geometry decreasing in size. In Figure 12 we show that while the size of the models in mode 1 decrease, the mapping error increases. Even though modes 2 and 3 still represent some changes in size, these changes have less effect on the overall volume of the heart and hence less influence on the mapping error. Modes 4 and higher, represent regional shape changes in the heart, that have little or no effect on the overall volume. Hence we observe that the mapping error in the ventricular regions stays constant throughout the instances representing −3 to +3 standard deviations from the mean shape. The mapping error

Author Manuscript Author Manuscript Author Manuscript Author Manuscript

in the intervalvular bridges shows the same trend, but a lot more variability, than observed for the ventricular regions.

5. Discussion

The topologically complex outflow tracts and valve annuli, contain clinically relevant regions for anatomically normal hearts and especially those with CHD. The inflow and outflow tracts can be the origin of arrhythmia in patients with and without structural heart diseases, making them crucial for anatomically correct computational models Cheung et al. (2019); Anderson et al. (2019); Aras et al. (2022). However, established ventricular coordinate systems do not automatically account for these regions Bayer et al. (2018); Schuler et al. (2021). The inclusion of these clinically important structures is essential when investigating regions of surgical interventions as for instance in patients with CHD, where regions of scar tissue and arrhythmia origins often manifest in these areas Kapel et al. (2017); Aras et al. (2022). Therefore, we created a tool to generate a biventricular coordinate system which automatically accounts for these highly variable regions to assist the investigation and understanding of myocardial dynamics and abnormalities.

The universal ventricular coordinates (UVC), an established ventricular coordinate system developed by Bayer et al. (2018), allow for the inclusion of the intervalvular bridges and detailed base by manual intervention. UVC have been shown to provide a robust tool, however a few characteristics of the method prove suboptimal. The final coordinates are determined by the solution to the Laplace equation and are prone to vary in heterogeneous geometries. Further, the final coordinates may not reflect the correct (normalized) distance potentially leading to inaccuracies in the resulting coordinatesSchuler et al. (2021).

A solution to include the inflow and outflow tracts without adding further discontinuities was suggested by Doste et al. (2019). Here, the authors also use the Laplace-Dirichlet system for their local coordinate system as proposed by Bayer et al. (2018), but in contrast to the UVC, they extend the apicobasal coordinate to take into account the four valve annuli. However, the solution to the Laplace equation does not provide the ideal properties for a robust coordinate system. Hence, this solution is not ideal for including the detailed base in a way that allows for subsequent granular analysis.

Another approach was suggested by the developers of the consistent biventricular coordinates Schuler et al. (2021). Their coordinate system is based on the trajectory distance method, which has been shown to result in a more consistent assignment of coordinates throughout varying geometries, as the method does scale better with distance even when local heterogeneities are present Schuler et al. (2021). However, Cobiveco only considers geometries with a flat base Schuler et al. (2021).

Therefore, we developed a method that combines the robustness of the trajectory distance method with the automated assignment of the anatomically detailed base. Our coordinate system CobivecoX is, to our knowledge, the first ventricular coordinate system to automatically include the highly variable intervalvular bridges, even in highly unusual anatomic pathologies. CobivecoX performs similarly in the complate biventricular geometry

Author Manuscript Author Manuscript Author Manuscript Author Manuscript

as previously published methods in truncated ventriclesSchuler et al. (2021); Bayer et al. (2018).

This tool will facilitate the inclusion and hence the study of the complex inflow and outflow tracts even in populations with challenging cardiac structures and a wide range of pathologies. By including and parametrizing these regions, CobivecoX enables mapping and statistically aggregating data close to the inflow and outflow tracts and comparison of important anatomical structures that may give rise to biomechanical changes and the origins of arrhythmia, in patients with and without structural heart disease Cheung et al. (2019); Anderson et al. (2019); Aras et al. (2022). Furthermore, CobivecoX enables the introduction of regions of interest as for instance surgical scars as present in CHD or regions of scar as commonly found in the anatomical base in myocardial infarction.

CobivecoX further provides tools to automatically assign the boundary surfaces required for calculating the local coordinates. Any user with a volumetric tetrahedral biventricular mesh can automatically calculate CobivecoX on their models to compare and validate data.

6. Limitations

CobivecoX can in the current implementation only be computed if the biventricular geometry has four valve annuli. CobivecoX is backwards compatible and recognizes biventricular shapes with a flat base. Even though we have demonstrated the use of CobivecoX on a single ventricle morphology, without further modification of the input landmarks, in the current implementation, CobivecoX cannot handle single ventricle morphologies like Pulmonary Atresia/Intact Ventricular Septum or Tricuspid Atresia, where one valve does not exist (Rao (2021)).

The separation of the intervalvular region from the ventricles leads to a discontinuity in the coordinate system that poses problems when using regression and interpolation based methods that could potentially be avoided by using sine or cosine transormations.

7. Conclusion

We created a ventricular coordinate system that automatically takes into account intervalvular bridges of the heart including the four valve annuli. The automated definition of the intervalvular bridges has been shown to work on a variety of cardiac morphologies. Compared with manual assignment of boundaries, CobivecoX facilitates reproducibility of coordinate assignment in different patients. With CobivecoX, we developed a system that performs similarly to previously published methods, while accounting automatically for more anatomical detail Schuler et al. (2021); Bayer et al. (2018) sufficient to describe the entire biventricular ventricular. We used and provide herewith a virtual cohort of CHD biventricular shapes based on a statistical atlas derived from patients with repaired TOF. The source code and the meshes are available online [software] Pankewitz and Hustad (2023) and [dataset] Pankewitz et al. (2023). CobivecoX can be readily applied to a variety of different geometries and has been shown to be applicable to various CHD pathologies.

Author Manuscript Author Manuscript Author Manuscript Author Manuscript

Supplementary Material

Refer to Web version on PubMed Central for supplementary material.

Acknowledgments

This work was supported by funding from the Research Council of Norway (303178) and NIH Grant HL121754. Mesh creation was run on resources provided by UNINETT Sigma2, the National Infrastructure for High Performance Computing and Data Storage in Norway. The authors would like to thank Aadarsh Bussooa, Laryssa Abdala, Katja Xu Haukebø Phillips and Noemi Zuercher for testing CobivecoX and improving the documentation, Axel Loewe and Steffen Schuler for scientific support and discussion about Cobiveco, and Jennifer Stowe for her coordination efforts in the McCulloch lab. ADM is a cofounder and equity holder of Insilicomed, Inc. and Vektor Medical Inc., neither of which has any relationship to this research.

References

Anderson RD, Kumar S, Parameswaran R, Wong G, Voskoboinik A, Sugumar H, Watts T, Sparks PB, Morton JB, McLellan A, et al. , 2019. Differentiating right-and left-sided outflow tract ventricular arrhythmias: classical ecg signatures and prediction algorithms. Circulation: Arrhythmia and Electrophysiology 12, e007392. [PubMed: 31159581]

Anderson RH, Mori S, Spicer DE, Brown NA, Mohun TJ, 2016. Development and morphology of the ventricular outflow tracts. World Journal for Pediatric and Congenital Heart Surgery 7, 561–577. [PubMed: 27587491]

Aras K, Gams A, Faye NR, Brennan J, Goldrick K, Li J, Zhong Y, Chiang CH, Smith EH, Poston MD, et al. , 2022. Electrophysiology and arrhythmogenesis in the human right ventricular outflow tract. Circulation: Arrhythmia and Electrophysiology 15, e010630. [PubMed: 35238622]

Bayer J, Prassl AJ, Pashaei A, Gomez JF, Frontera A, Neic A, Plank G, Vigmond EJ, 2018. Universal ventricular coordinates: A generic framework for describing position within the heart and transferring data. Medical Image Analysis 45, 83–93. URL: 10.1016/j.media.2018.01.005, doi:10.1016/j.media.2018.01.005. [PubMed: 29414438]

Cheung JW, Anderson RH, Markowitz SM, Lerman BB, 2019. Catheter ablation of arrhythmias originating from the left ventricular outflow tract. JACC: Clinical Electrophysiology 5, 1–12. [PubMed: 30678772]

Doste R, Soto-Iglesias D, Bernardino G, Alcaine A, Sebastian R, Giffard-Roisin S, Sermesant M, Berruezo A, Sanchez-Quintana D, Camara O, 2019. A rule-based method to model myocardial fiber orientation in cardiac biventricular geometries with outflow tracts. International journal for numerical methods in biomedical engineering 35, e3185. [PubMed: 30721579]

Geuzaine C, Remacle JF, 2009. Gmsh: A 3-D finite element mesh generator with built-in pre- and post-processing facilities. International Journal for Numerical Methods in Engineering 79, 1309–1331. URL: 10.1002/nme.2579, doi:10.1002/nme.2579.

van Gils FA, 1981. The fibrous skeleton in the human heart: embryological and pathogenetic considerations. Virchows Archiv A 393, 61–73.

Govil S, Mauger C, Hegde S, Occleshaw CJ, Yu X, Perry JC, Young AA, Omens JH, McCulloch AD, 2023. Biventricular shape modes discriminate pulmonary valve replacement in tetralogy of fallot better than imaging indices. Scientific Reports 13, 2335. [PubMed: 36759522]

Hickey EJ, Veldtman G, Bradley TJ, Gengsakul A, Manlhiot C, Williams WG, Webb GD, McCrindle BW, 2009. Late risk of outcomes for adults with repaired tetralogy of fallot from an inception cohort spanning four decades. European Journal of cardio-thoracic Surgery 35, 156–164. [PubMed: 18848456]

Kapel GF, Sacher F, Dekkers OM, Watanabe M, Blom NA, Thambo JB, Derval N, Schalij MJ, Jalal Z, Wijnmaalen AP, et al. , 2017. Arrhythmogenic anatomical isthmuses identified by electroanatomical mapping are the substrate for ventricular tachycardia in repaired tetralogy of fallot. European heart journal 38, 268–276. [PubMed: 28182233]

Kirby ML, Waldo KL, 1995. Neural crest and cardiovascular patterning. Circulation research 77, 211–215. [PubMed: 7614707]

Author Manuscript Author Manuscript Author Manuscript Author Manuscript

Kirklin JK, Kirklin JW, Blackstone EH, Milano A, Pacifico AD, 1989. Effect of transannular patching on outcome after repair of tetralogy of fallot. The Annals of thoracic surgery 48, 783–791. [PubMed: 2596914]

Mauger CA, Govil S, Chabiniok R, Gilbert K, Hegde S, Hussain T, McCulloch AD, Occleshaw CJ, Omens J, Perry JC, et al. , 2021. Right-left ventricular shape variations in tetralogy of fallot: associations with pulmonary regurgitation. Journal of Cardiovascular Magnetic Resonance 23, 1–14. [PubMed: 33390185]

Niederer S, Aboelkassem Y, Cantwell CD, Corrado C, Coveney S, Cherry EM, Delhaas T, Fenton FH, Panfilov A, Pathmanathan P, et al. , 2020. Creation and application of virtual patient cohorts of heart models. Philosophical Transactions of the Royal Society A 378, 20190558.

Niederer SA, Lumens J, Trayanova NA, 2019. Computational models in cardiology. Nature Reviews Cardiology 16, 100–111. [PubMed: 30361497]

Pankewitz L, Hustad KG, 2023. Cobivecox. URL: https://github.com/lisapankewitz/Cobiveco.

Pankewitz L, Hustad KG, Govil S, Perry JC, Hegde S, Tang R, Omens JH, Young AA, McCulloch AD, Arevalo HJ, 2023. Cobivecox - dataset. doi: 10.5281/zenodo.7922601.

Peirlinck M, Costabal FS, Yao J, Guccione J, Tripathy S, Wang Y, Ozturk D, Segars P, Morrison T, Levine S, et al. , 2021. Precision medicine in human heart modeling. Biomechanics and modeling in mechanobiology 20, 803–831. [PubMed: 33580313]

Rao PS, 2021. Single ventricle—a comprehensive review. Children 8, 441. [PubMed: 34073809]

Schuler S, Pilia N, Potyagaylo D, Loewe A, 2021. Cobiveco: Consistent biventricular coordinates for precise and intuitive description of position in the heart – with MATLAB implementation. Medical Image Analysis 74, 102247. URL: 10.1016/j.media.2021.102247, doi:10.1016/j.media.2021.102247. [PubMed: 34592711]

Author Manuscript Author Manuscript Author Manuscript Author Manuscript

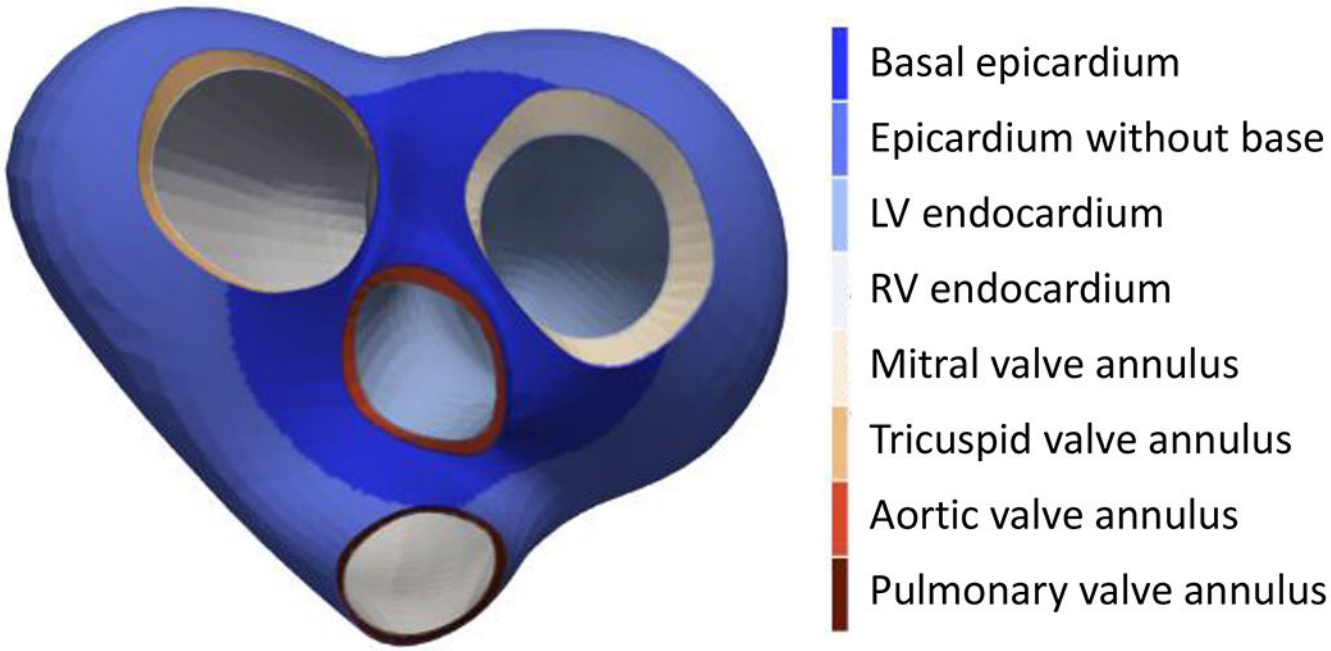

Fig. 1.

Boundary surfaces needed as input for CobivecoX include an epicardial surface with base, epicardial surface without base, the LV Endocardium, the RV endocardium, the mitral valve annulus, the tricuspid valve annulus, the aortic valve annulus and pulmonary valve annulus.

Author Manuscript Author Manuscript Author Manuscript Author Manuscript

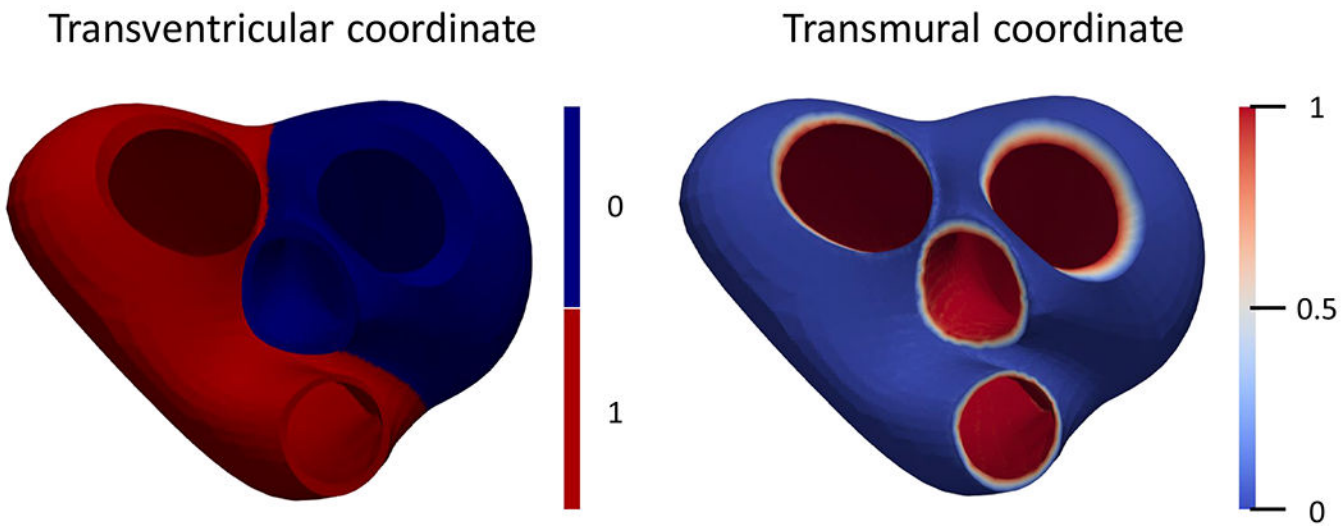

Fig. 2.
Transventricular and transmural coordinate on the atlas mean shape.

Author Manuscript Author Manuscript Author Manuscript Author Manuscript

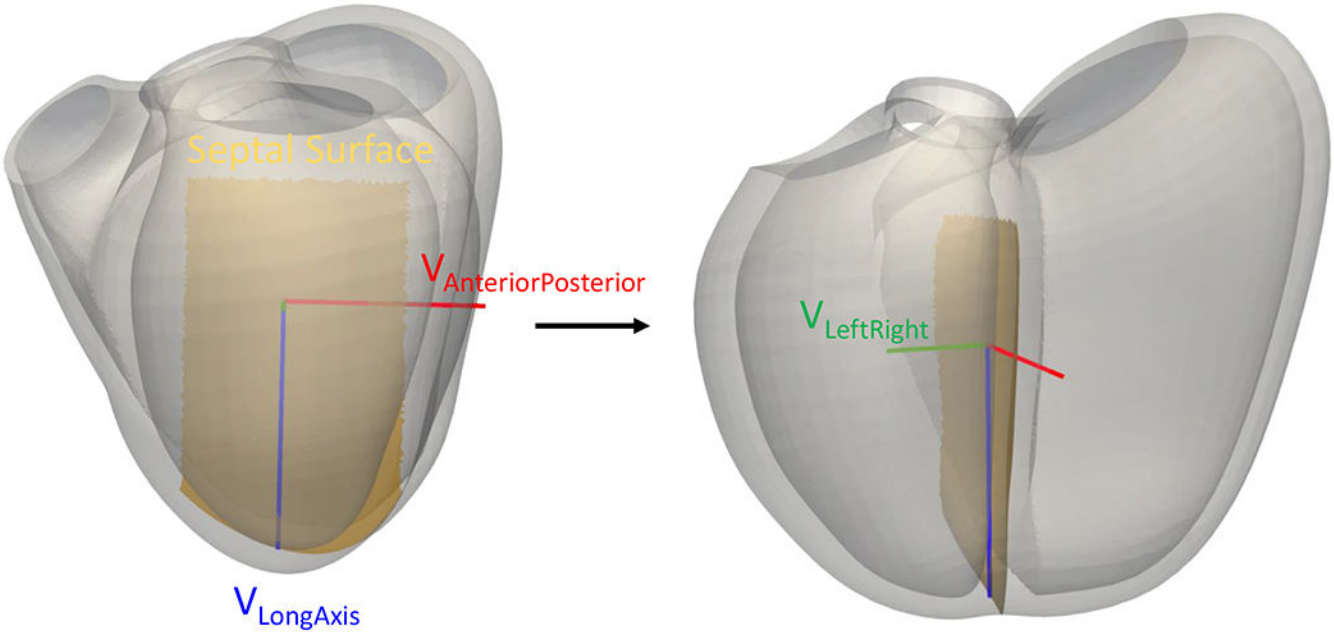

Fig. 3.

Truncated septal surface shown in dark yellow. In addition to the previously described truncations in the posterior anterior trajectory (Schuler et al., 2021), an additional truncation in the trajectory of $v_{LongAxis}$ is applied at the basal side. The three global heart axes $v_{LongAxis}$, $v_{AnteriorPosterior}$ and $v_{LeftRight}$, are shown in blue, red and green, respectively.

Author Manuscript Author Manuscript Author Manuscript Author Manuscript

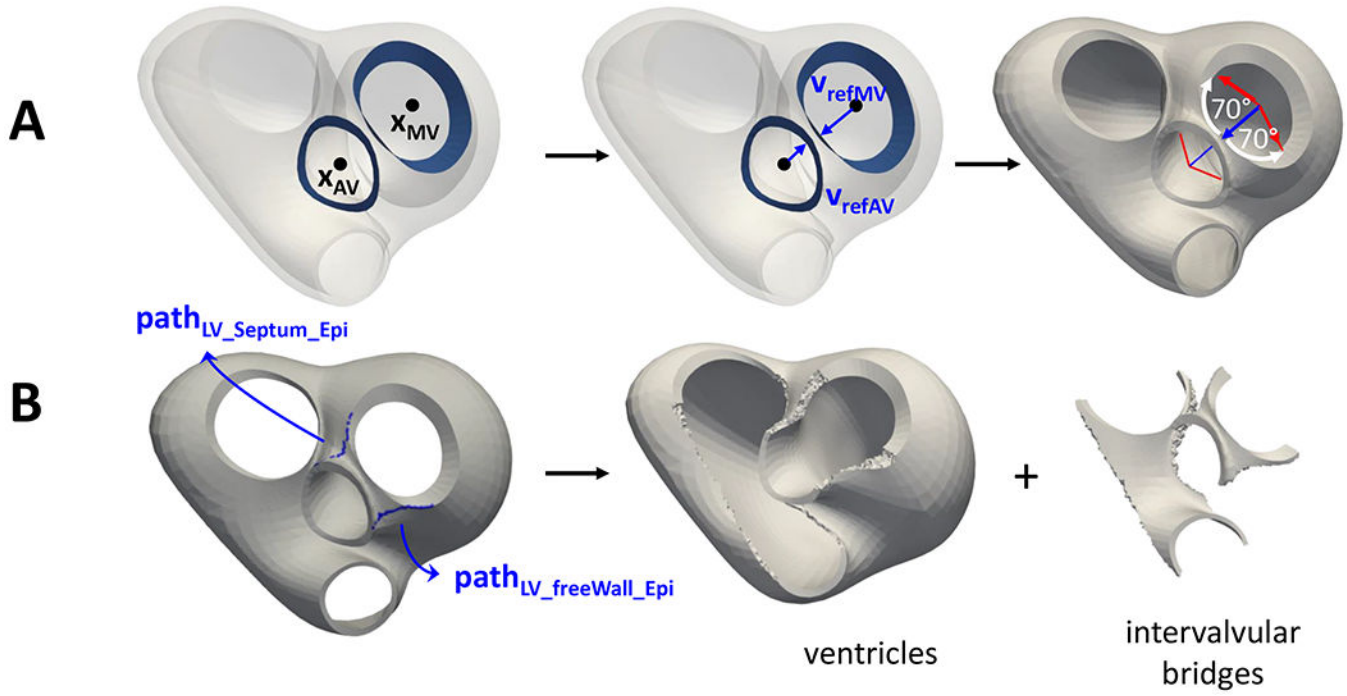

Fig. 4.

Workflow for dividing the mesh into ventricles and intervalvular bridges. Scheme nonly shows the left ventricle. The workflow follows the same steps in the right ventricle. (A) First, the center of the valve annuli surfaces are calculated. Then the vector connecting the center points in the respective ventricle is calculated. A reference vector is calculated in each annulus respectively (upper row, middle). The reference vector is rotated around the surface normal clockwise and counter-clockwise, yielding two rotated vectors (A, right). Based on the rotated reference vectors, two points on the respective annulus are defined referred to as starting points. (B) A graph taking into account the surface nodes and edges describing the respective ventricle (excluding the septum) is created. In this graph, the four starting points in the respective ventricle are used to define the two shortest path between the inflow and outflow valve annuli which are in the LV reresented by $path_{LVSeptumEndo}$ and $path_{LVfreeWallEndo}$ on the endocardial surface. Next, a graph representing the epicardial surface mesh is created. In this graph, the nodes with the shortest distance to the two defined path in the LV endocardium are calculated. This yields two paths in each ventricle. The paths in the epicardial and endocardial graph are used to define two planes, one at the septal and one at the free wall side of the intervalvular bridges. The planes are used as cutting planes, separating the intervalvular bridges from the ventricles. For increased visibility we recommend the digital version of this figure.

Author Manuscript Author Manuscript Author Manuscript Author Manuscript

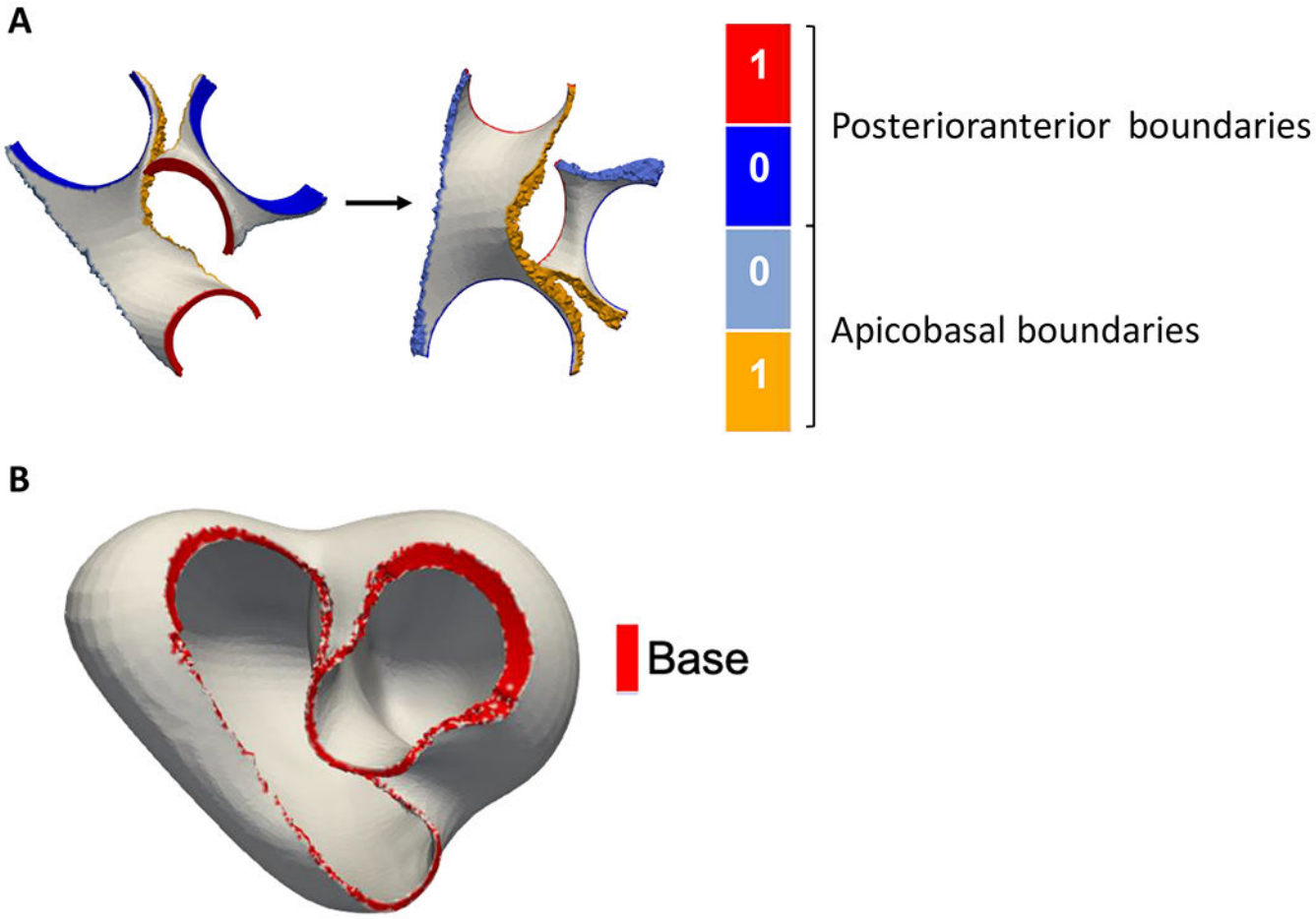

Fig. 5.

Definition of boundary surfaces on the (A) intervalvular bridges. Boundaries for defining inflow-outflow and apicobasal coordinate are color coded. (B) Definition of boundary surfaces on the ventricles. After removing the intervalvular bridges from the ventricles a new base is defined as a surface boundary.

Author Manuscript Author Manuscript Author Manuscript Author Manuscript

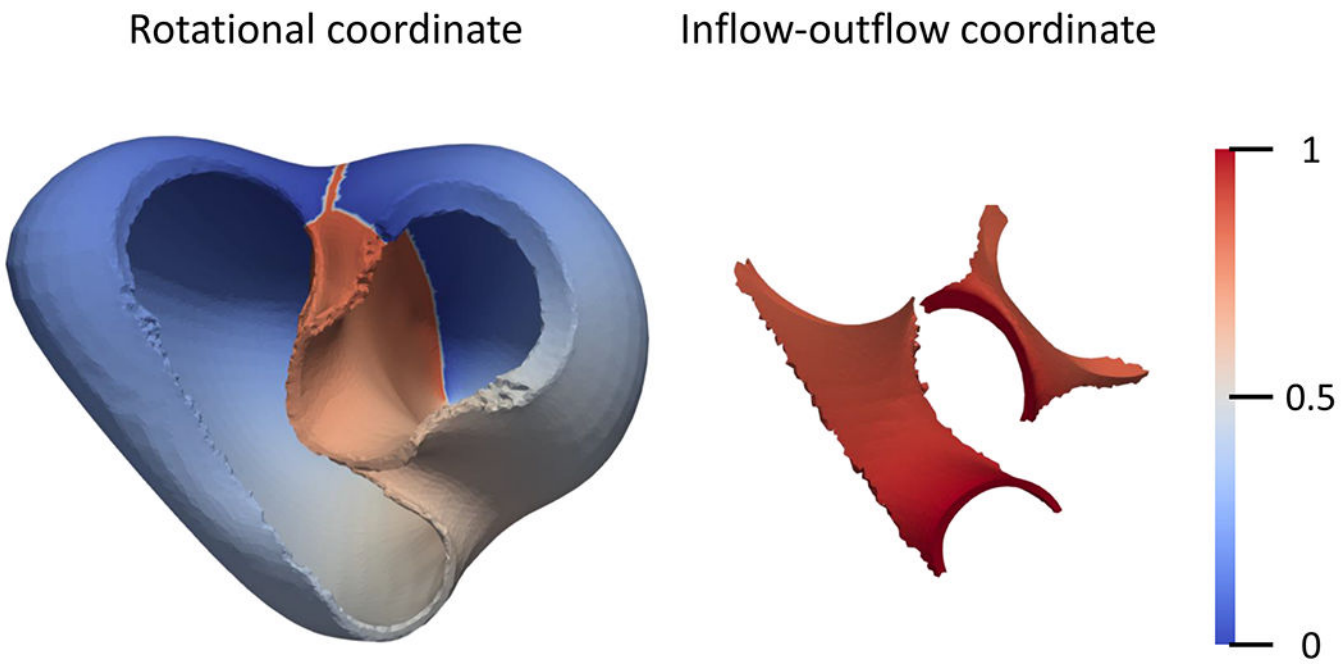

Fig. 6.
Rotational coordinate and inflow-outflow coordinate on the atlas mean shape. Same color scale used for both.

Author Manuscript Author Manuscript Author Manuscript Author Manuscript

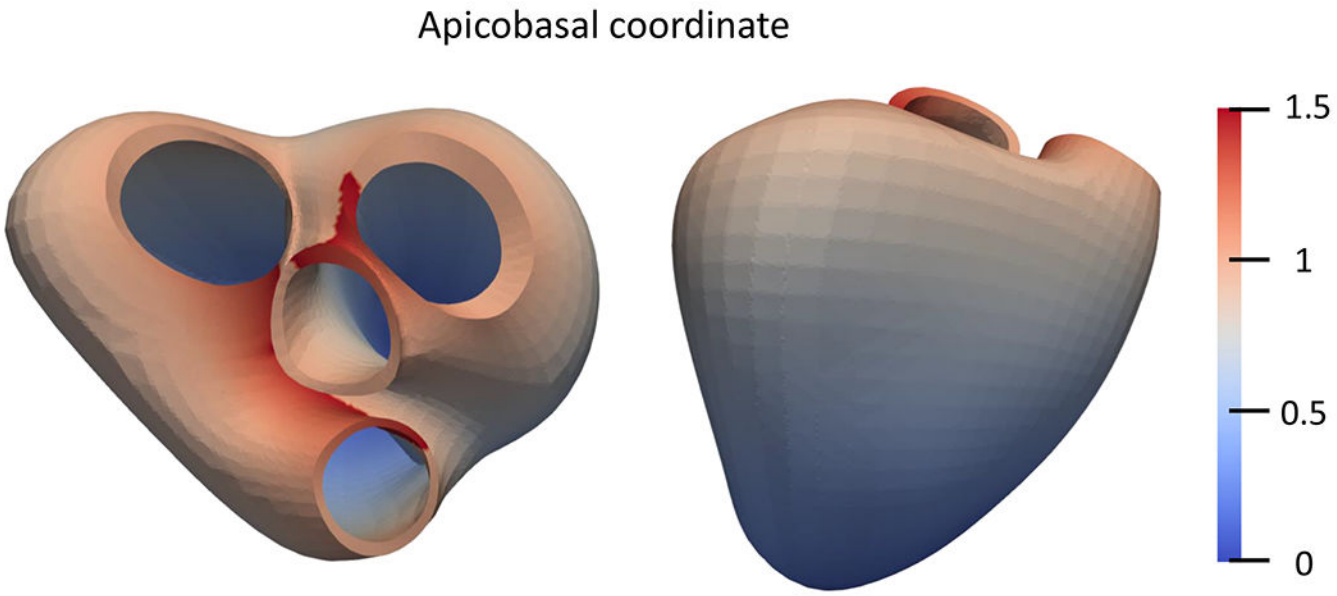

Fig. 7.
Apicobasal coordinate on the atlas mean shape.

Author Manuscript Author Manuscript Author Manuscript Author Manuscript

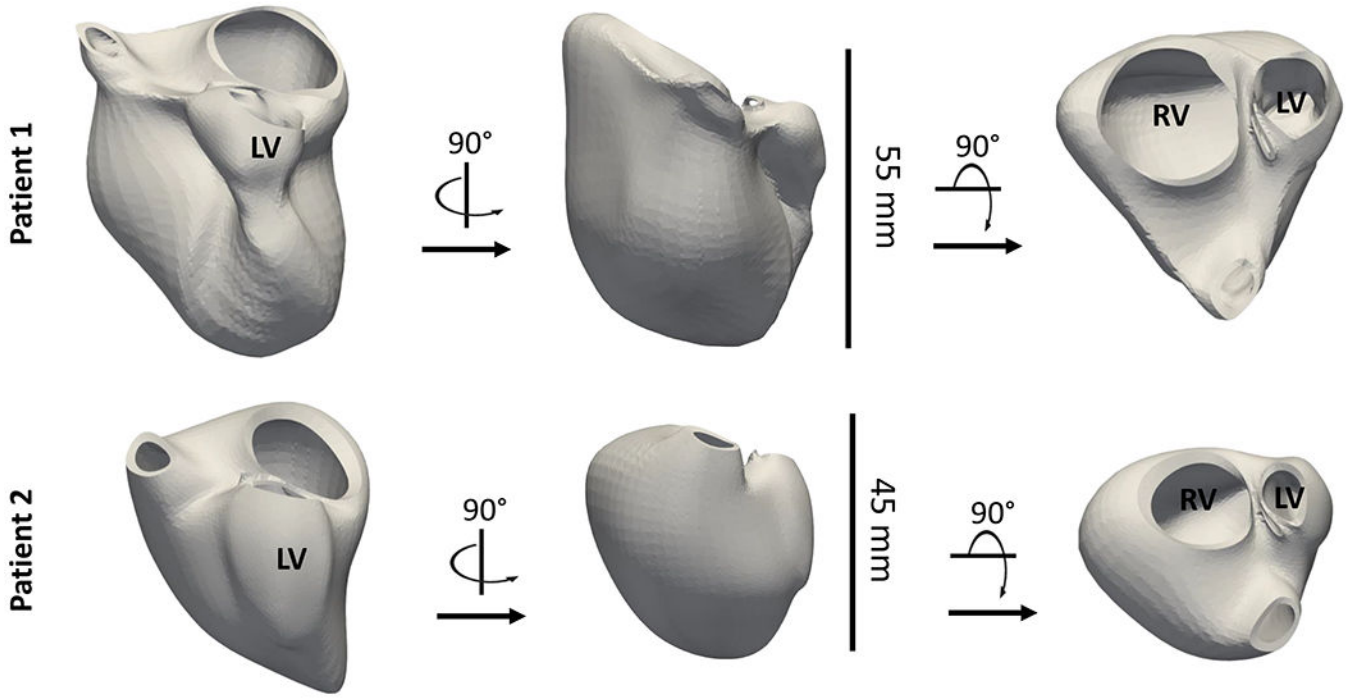

Fig. 8.

Patient specific meshes of the HLHS patients. The vertical bars show the size of the patients heart for comparison.

Author Manuscript Author Manuscript Author Manuscript Author Manuscript

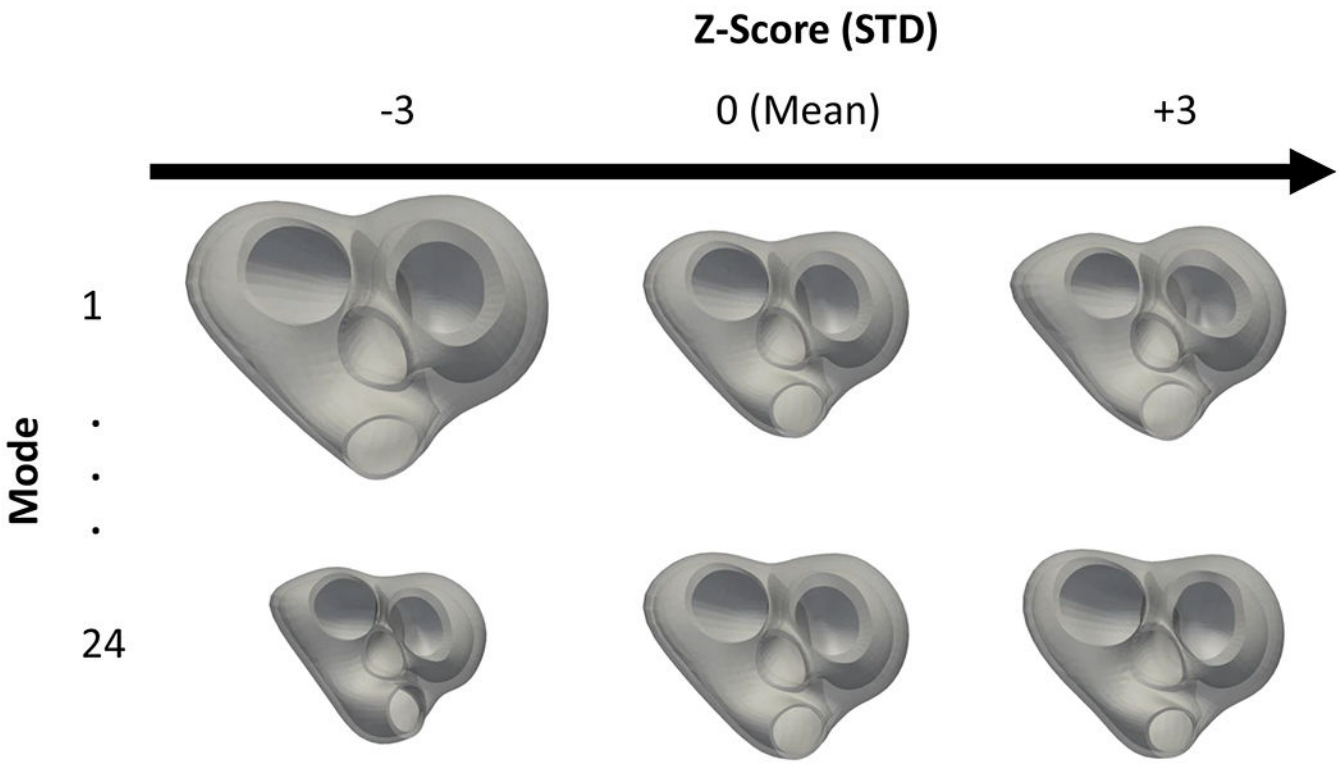

Fig. 9.
Example visualization of −3 and +3 Z-Score geometries in modes 1 and 24.

Author Manuscript Author Manuscript Author Manuscript Author Manuscript

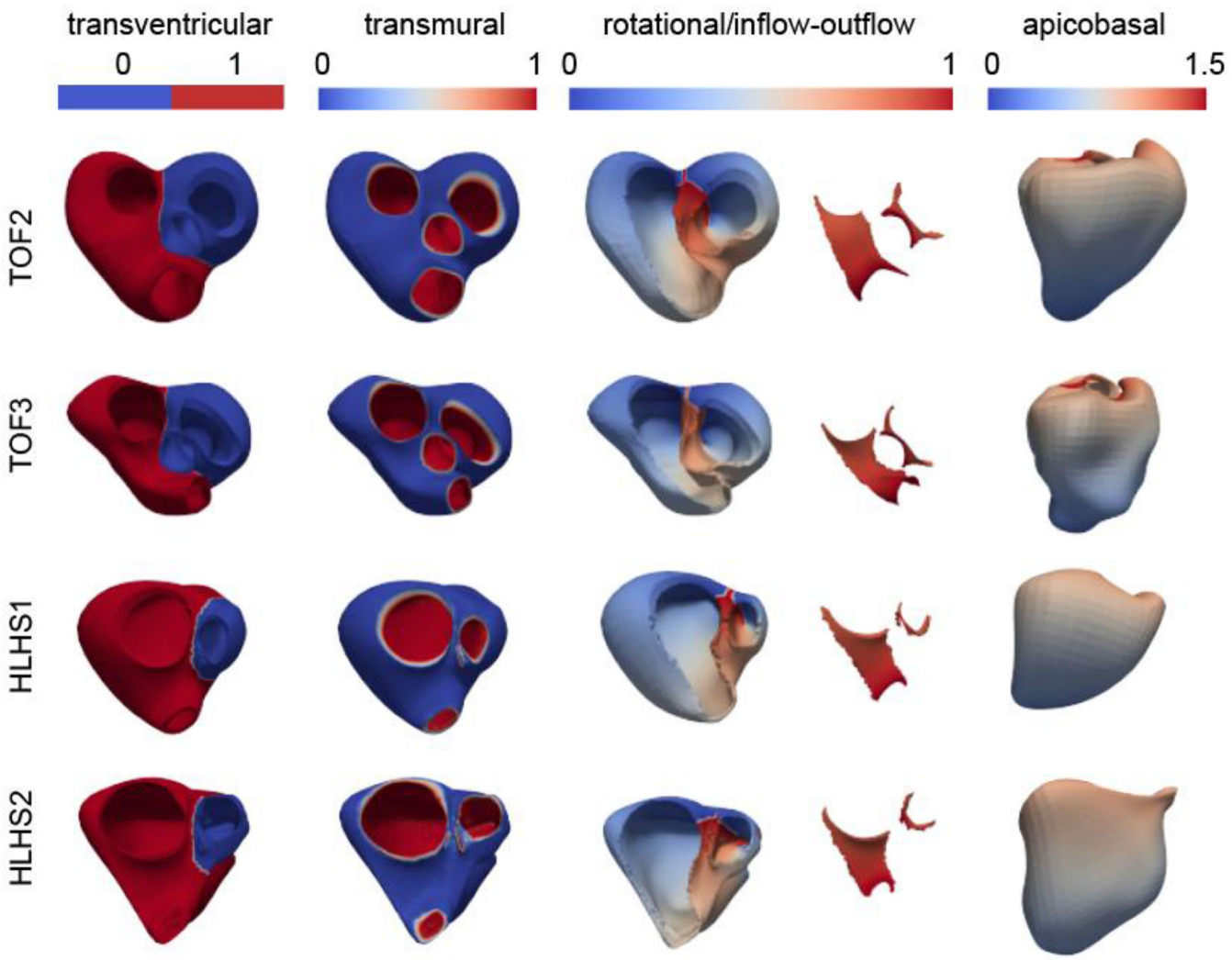

Fig. 10.

Examples of TOF and HLHS cohort with assigned CobivecoX coordinates. Each row represents a patient and each column a coordinate. Coordinates are unitless.

Author Manuscript Author Manuscript Author Manuscript Author Manuscript

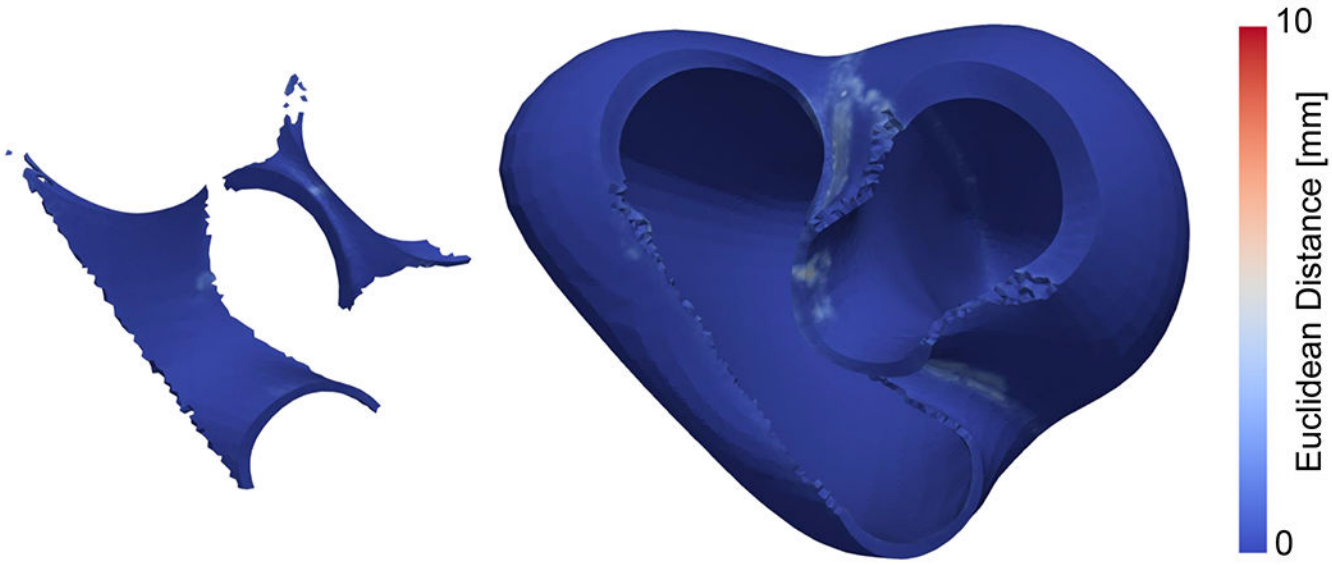

Fig. 11.

Mean two-way mapping error distribution represented by the Euclidean distance in mm in the TOF atlas cohort on the mean TOF shape.

Author Manuscript Author Manuscript Author Manuscript Author Manuscript

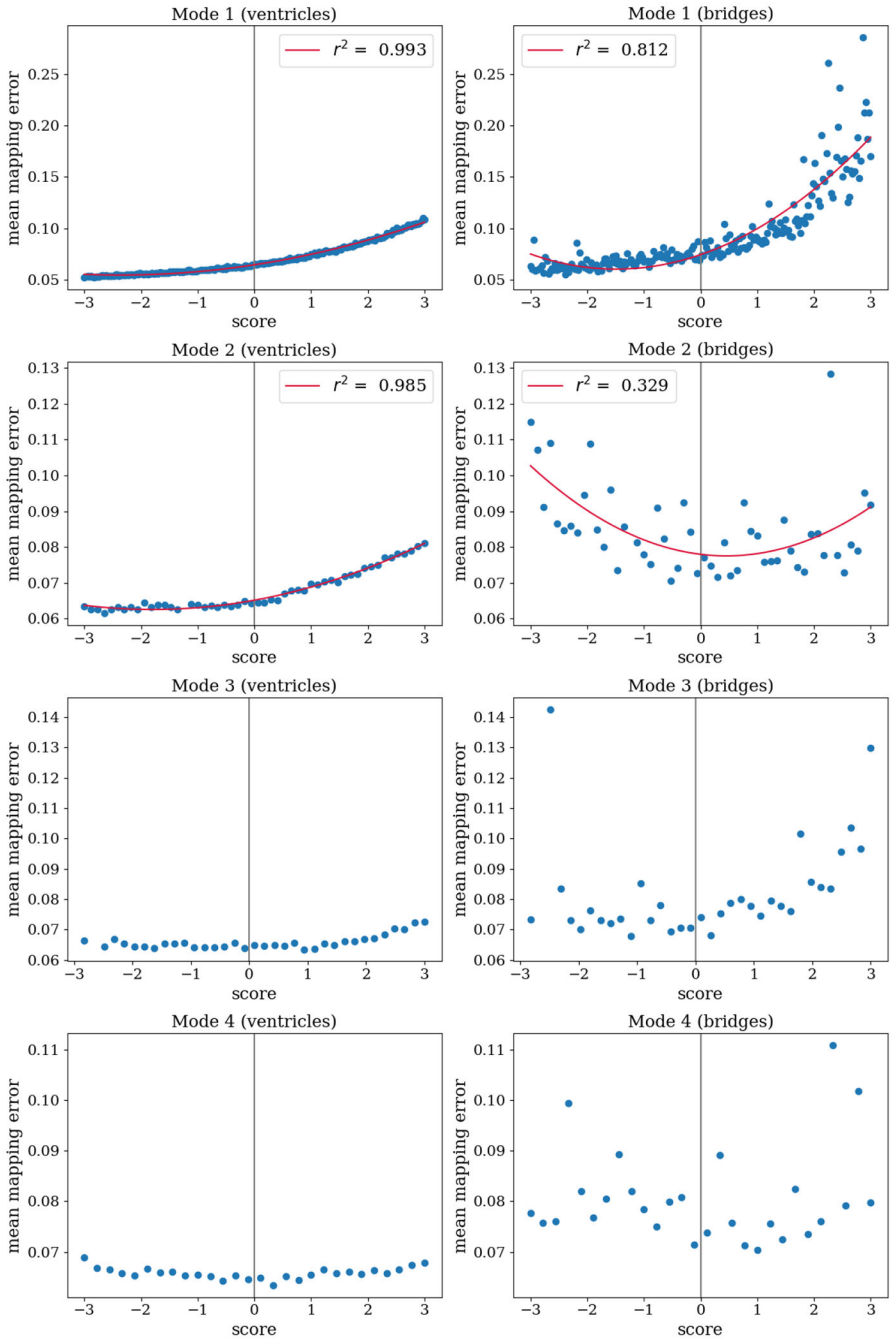

Fig. 12.

Visualization of weighted scores against mean two-way mapping error (referred to as mean mapping error) in the respective TOF atlas mode. The first column shows the errors observed in the ventricular region. The second column refers to the mean two-way errors in the interventricular (referred to as bridge) bridges. Each row refers to a different mode. For brevity, only modes 1 to 4 are shown.

Author Manuscript Author Manuscript Author Manuscript Author Manuscript

Table 1.

Two-way mapping error. All values in mm.

System	Population	Area	Median	Mean	90th P	99th P
CobivecoX	CHD Atlas n=481	biventricular geometry	0.02	0.07	0.12	1.0
	TOF Patient specific geometries n=9		0.02	0.08	0.14	1.18
	HLHS Patient specific geometries n=2		0.08	0.3	0.58	4.37
Cobiveco 1.0	Patient specific geometries cohort (Schuler et al. (2021))	truncated ventricles	0.013	0.038	0.084	0.385
UVC	Patient specific geometries cohort (Schuler et al. (2021))	truncated ventricles	0.007	0.134	0.164	2.944